

## FORMULATION AND EVALUATION OF POLYMERIC NANOSUSPENSION OF NARINGENIN

R. SUMATHI\*, S. TAMIZHARASI, T. SIVAKUMAR

Nandha College of Pharmacy and Research Institute, Erode 630052, Tamilnadu, India

Email: sumoraji@gmail.com

Received: 28 Jul 2017, Revised and Accepted: 10 Oct 2017

### ABSTRACT

**Objective:** The objective of this study was to formulate and evaluate the poorly soluble drug, naringenin (NAR) into nanosuspension to increase the solubility and enhance the dissolution rate and then improve its bioavailability.

**Methods:** Nanosuspension of naringenin (NARNS) was prepared using high-pressure homogenization method using Soya lecithin, Polaxamer-407, Polaxamer-188, Hydroxypropyl methyl cellulose (HPMC) and Tween-80. Ten formulations were prepared to show the effect of stabilizer and its ratio. D- $\alpha$ -Tocopheryl polyethylene glycol succinate 1000 (TPGS) was added as a co-stabilizer. All these formulations were evaluated for their particle size, PDI, zeta potential, FT-IR study, drug content, saturation solubility studies, entrapment efficiency, *in vitro* permeability and *in vitro* drug release. The formulation was further evaluated for scanning electron microscope (SEM), differential scanning calorimetry (DSC) and Powder X-ray diffraction (P-XRD) and hemocompatibility assessment.

**Results:** All the prepared formulations were in the nano size. The optimum concentration of the stabilizer was in the formulation was found 1:1.5:1 (drug: stabilizer: co-stabilizer ratio). Dramatic effect of the particle size reduction was found by the addition of the co-stabilizer (TPGS) in formulation N2 that has P. S  $80.52 \pm 0.13$  nm. The solubility and dissolution of NAR in the form of NARNS were significantly higher than those of pure NAR. SEM report shows that naringenin nanosuspension revealed a smooth texture. P-XRD crystallography diffraction and DSC studies indicated that the crystalline state of NAR was converted into amorphous nature. The safety evaluation showed that NARNS provided a lower rate of erythrocyte hemolysis.

**Conclusion:** In this study, (NARNS) was successfully carried out by high-pressure homogenization technique and characterized. The physico-chemical characterization shown that crystalline naringenin was converted to a polymorphic form (DSC and P-XRD Study) which evidenced by enhanced dissolution rate in comparisons of the formulation with (NAR) pure drug. The NARNS has shown  $7.5 \pm 0.4$  fold increased relative bioavailability when compared to the NAR. The increased drug dissolution rate may have a significant impact in absorption which in turn the improved oral bioavailability of naringenin. Thus, this delivery system may prefer to improve the dissolution of poorly soluble drugs like NAR and thus enhanced oral bioavailability. The safety evaluation showed that nanoformulation (NF2) shows a lower rate of erythrocyte hemolysis. These findings suggest that the selected formulation may represent a promising new drug formulation for intravenous administration in the treatment of certain cancers.

**Keywords:** Naringenin, High-Pressure Homogenization, Nanosuspension, Solubility, Bioavailability

© 2017 The Authors. Published by Innovare Academic Sciences Pvt Ltd. This is an open access article under the CC BY license (<http://creativecommons.org/licenses/by/4.0/>)  
DOI: <http://dx.doi.org/10.22159/ijap.2017v9i6.21674>

### INTRODUCTION

Cancer is a group of diseases that cause cells throughout the body to change and grow out of control. Most types of cancer cells eventually form a lump or mass called a tumor, and are named after the part from the body where the tumor originates. Cancer is one of the leading causes of death worldwide, which has been attributed to many factors that have influenced the increase on the number of cases. Some of the direct factors include the growth as the population, aging, and adoption of lifestyle behaviors that are known to cause cancer [1]. According to world health organization, more than 57 million deaths have occurred in 2008. Of which, 36 million (63 %) deaths were due to non-communicable diseases such as cardiovascular diseases, diabetes and cancer [2]. Of all non-communicable diseases, with more than 7.6 million deaths, cancer ranked third as the leading cause of death worldwide. The current statistics suggest that the cancer prevalence will continue to rise and may reach around 17 million cancer deaths by 2030 [3, 4]. The major therapeutic approaches to the treatment of both localized and metastasized cancer in chemotherapy, which are being used alone or in a combination of other forms of cancer therapies [5]. However, the use of chemotherapeutic drugs is limited by high toxicity, rapid elimination from the systemic circulation, accumulation in non-targeted organs and tissues, enzymatic and hydrolytic degradation and/or inefficient cell entry. Thus, the inhibition of tumor cell growth without side effects is recognized as an important target for cancer therapy. Dietary flavonoids are a widely distributed group of diphenolic compounds of plant origin. Epidemiological studies have consistently shown an inverse association between consumption of some nutritional flavonoids and the risk of human cancers at many

sites [6-9]. NAR has been widely studied and has been reported to be an antioxidant [10, 11], NAR, and the aglycone of naringin was found to exhibit aorta anti-ulcer effects [12], antioxidant [13] and dilatory as well as inhibiting the proliferation of breast cancer and delaying mammary tumorigenesis. Fig. (1) Shows the chemical structure of naringenin [14].

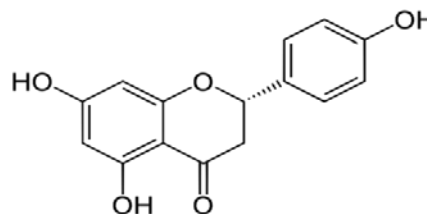


Fig. 1: Chemical structure NAR

Regretfully, the clinical relevance of NAR is limited by its low solubility and minimal bioavailability owing to its largely hydrophobic ring structure. In addition, NAR had unfavourable body distribution and inability to cross-cellular barriers. Therefore NARNS was developed to overcome major obstacles associated with NAR bioavailability. One of the ways to improve the selectivity and effectiveness of nanoparticle delivery system is by conjugating nanoparticles to molecules that could specifically reach target cancer cells [15]. Nanotechnology is the control as a matter at

dimensions of roughly 1 to 100 nm, providing unique properties of the matter because of its small size. Nanotechnology offers many benefits in medicine such as protecting drugs from degradation, enhancing solubility of water-insoluble or poorly soluble drugs as well as increasing efficiency of an active ingredient. These benefits help to reduce drug doses which in turn decrease the risk of its side effect and toxicity [16]. The aim of present study was to formulate the NARNS in order to improve its solubility and enhance *in vitro* dissolution rate.

## MATERIALS AND METHODS

### Materials

NAR was purchased from Zim laboratories Limited, Nagpur. Soya lecithin was purchased from Glenmark generics limited Mumbai, India. Polaxamer-188 and Polaxamer-407 were provided by Dr. Reddy's Generics. TPGS was obtained from Ludwigshafen, Germany. Tween-80 was obtained from Nice chemicals limited, Cochin. All other chemicals and the solvents were of analytical reagent grade, and deionized water was used for this study. The experimental protocol was approved by the Institutional animal ethics committee (IAEC) of CPCSEA (Committee for the Purpose of Control and Supervision of Experiments on Animals), (NCP/IAEC/2015-16-04).

### Methods

#### Determination of $\lambda_{\max}$

10 mg of NAR were dispersed in 100 ml 0.1N HCl pH 1.2 to prepare 0.1 mg/ml stock solution. From this stock solution, a dilute (10  $\mu\text{g/ml}$ ) solution was prepared and scanned by UV spectrophotometer at the range of 200-400 nm, the same steps were repeated with phosphate buffer pH 7.4 to obtain the  $\lambda_{\max}$  of NAR in these medium [17].

### Preparation of calibration curves

Calibration curves of NAR in 0.1 N HCl pH 1.2 and phosphate buffer pH 7.4 were constructed by preparing serial dilutions of the drug from 0.1 mg/ml stock solution for each medium. The prepared samples were analyzed spectrophotometrically at  $\lambda_{\max}$  in these media. The plot of absorbance vs. concentration is done and Beer's range was determined [18]. The results were analyzed in triplicate, and the standard deviation was represented.

### Fourier transform Infra-red spectroscopy

FT-IR spectra were recorded in the sample prepared in KBr disks (2 mg sample in 200 mg KBr disks) using Shimadzu Fourier Transform Infra-Red spectrometer. The samples were scanned over a frequency range 4000-400  $\text{cm}^{-1}$  [19].

### Formulation of naingnin nanosuspension

NARNS was prepared by high pressure homogenization technique by using the different concentration of the stabilizers like Soya lecithin (N1 and N2) poloxamer 407 (N3 and N4), poloxamer 188 (N5 and N6), Hydroxypropyl methyl cellulose (HPMC) (N7 and N8) and Tween-80 (N9 and N10) with (0.75 % and 1.5 %) and TPGS (1%) respectively, but in all the drug concentration remains constant. NAR powder (1 % w/v) was dispersed in aqueous surfactant solution using magnetic stirrer. After drug dispersion in the surfactant solution first size reduction step was carried out using an Ultra-Turax T25 basic homogenizer at 9500 rpm for 10 min. The obtained mixtures were homogenized using Micron-LAB 40 high-pressure homogenizer, the homogenization step includes first two cycles at 100 bar and next two cycles at 500 bars pressure as an initial step. Finally, the suspension was homogenized for 15 cycles at 1500 bar pressure [20].

Table 1: Composition of NARNS

Code	Drug: Polymer: TPGS ratio
N1	1:0.75:1 (Nar: Soya lecithin: TPGS)
N2	1:1.5:1 (Nar: Soya lecithin: TPGS)
N3	1:0.75:1 (Nar: Polaxamer407: TPGS)
N4	1:1.5:1 (Nar: Polaxamer407: TPGS)
N5	1:0.75:1 (Nar: Poloxamer188: TPGS)
N6	1:1.5:1 (Nar: Poloxamer188: TPGS)
N7	1:0.75:1 (Nar: HPMC: TPGS)
N8	1:1.5:1 (Nar: HPMC: TPGS)
N9	1:0.75:1 (Nar: Tween-80: TPGS)
N10	1:1.5:1 (Nar: Tween-80: TPGS)

The homogenized nanosuspensions were freeze-dried to increase the shelf life of suspension and to study the dissolution behaviour. 1% mannitol was added to each formulation as a cryoprotectant at the time of lyophilization. Virtis freeze drier is used for lyophilization of nanosuspension. At first, the sample was kept overnight in deep freezer at -70 °C and then the sample was kept in Virtis freeze drier for two d at -50 °C at 2 millitorr [21].

### Particle size distribution and polydispersity index

The particle size analysis of different batches of nanosuspension was carried out using Microtac Blue wave-particle size analyzer. Before measurement of the samples, they have to be diluted with de-ionized water to obtain a suitable concentration for measurement. The results obtained for particle size distributions were used to confirm the formation of nano-sized particles [22].

### Zeta potential analysis

The particle charge was one of the most important parameters in assessing the physical stability of emulsion and suspensions. The large numbers of particles were equally charged; then electrostatic repulsion between the particles was increased, and thereby physical stability of the formulation was also increased. Typically, the particle charge of the colloidal system was measured as zeta potential via the electrophoretic mobility of the particles in an electrical field. Zeta potential analysis of prepared nanosuspension formulation was

carried out using Malvern Zetasizer (Malvern Instruments). Before measurement, the samples were diluted with de-ionized water, and conductivity was adjusted by addition of sodium chloride [22].

### Re-dispersibility and percentage drug content determination

The NARNS were analyzed for drug content by UV spectroscopic method. Different batches of nanosuspension equivalent to 10 mg of NAR weighed accurately and dissolved in 10 ml methanol. The stock solutions were diluted with distilled water and analyzed by UV spectroscopy at 290 nm [23].

### Determination of entrapment efficiency (EE) of nanosuspension

10 ml of nanosuspension was centrifuged at 5000 rpm for 20 min. The supernatant solution was filtered and separated. One ml of these filtrates was diluted with water and the absorbance at maximum  $\lambda_{\max}$  was measured by UV spectrophotometer using water as blank [24]. The amount of free drugs in the formulations was measured and the entrapment efficiency is then calculated.

### Saturation solubility studies

The saturation solubility studies were carried out for both the unprocessed pure drug and different batches of lyophilized nanosuspension. 10 mg of unprocessed pure drug and nanosuspension equivalent to 10 mg of NAR was weighed and separately introduced into 25 ml stopper conical flask containing 10

ml distilled water. The flasks were sealed and placed in rotary shaker for 24 h at 37 °C and equivalent for 2 d. The samples were collected after the specified time interval, and it is filtered and analyzed. The samples were analyzed using UV spectrophotometer at 290 nm [25].

#### In vitro drug release studies

The *in vitro* release of NAR drug and its NARNS were carried out in USP dissolution test apparatus using paddle method at a rotation speed of 50 rpm. The dissolution profile was carried out in the freshly prepared acidic buffer (pH 1.2) and also in the phosphate buffer (pH 7.4). 10 mg of pure drug and nanosuspension containing 10 mg of naringenin equivalent was taken and placed in the dissolution mediums. The volume and temperature of dissolution medium were 900 ml and 37.0±0.2 °C, respectively. Samples were withdrawn at fixed time intervals and were filtered. The filtered samples were analyzed at 290 nm using Shimadzu UV-Visible spectrophotometer. The results obtained for different batches of the formulation were compared to the dissolution profile of NAR [25, 26].

#### In vitro permeation studies

Permeation study was carried out for both unprocessed drug and different batches of nanosuspension using cellulose nitrate membrane. The membrane was attached to the diffusion cell, and then it was dipped in a beaker containing phosphate buffer pH 7.4. The pure drug sample and equivalent quantities of lyophilized nanosuspension were weighed and placed in the different diffusion cell containing the specific quantity of buffer. The samples were withdrawn at specific time intervals for 1 hr and replaced with fresh buffer solution. Finally, the samples were analyzed using UV spectrophotometer at 290 nm [27].

#### Differential scanning calorimetry

Thermal properties of formulations were analyzed by differential scanning calorimetric analysis using Toledo-DSC II. To characterize the changes in internal structure DSC analysis was carried out for NAR, polymer and the lyophilized NARNS. The 5 mg of sample was taken in the aluminum vial and kept in the instrument. The sample was then heated from 20 °C to 200 °C at a heating rate of 10 °C/min under a stream of nitrogen at a flow rate of 50 ml/min. Enthalpy changes ( $\Delta H$ ) were calculated peak to study the polymeric changes in the formulations [28].

#### Scanning electron microscopy

The scanning electron microscopy (SEM) is one of the most important instruments used for analysis of surface morphology. The particle size analysis of lyophilized NARNS was carried out to confirm the nanosized of the formulation. The samples are lightly sprinkled on a double side adhesive tape stuck to an aluminium stub, and the stubs were coated with platinum. The stub containing sample is placed in SEM chamber and analyses the surface morphology [29].

#### Powder X-ray diffraction pattern

The P-XRD studies of nanosuspension were carried out using X-ray diffractometer with copper (Cu) as target filter having a voltage/current of 40KV/40 Ma at a scan speed of 1 °/min. The samples were analyzed at a 2 $\theta$  angle range of 5-70 ° [30, 31].

#### Stability study

Stability studies were carried out for naringenin nanosuspension formulation as per ICH guidelines. The best NARNS (N2) was sealed in high-density polyethylene bottles and stored at 4±1 °C/Ambient, 25±2 °C/60±5 % RH %, 40±2 °C/75±5 % RH for 90 d. The samples were evaluated for percentage naringenin nanosuspension. [32].

#### Hemocompatibility assessment

##### Whole blood cell lysis

Blood was collected in heparinized tubes from Wistar rats and centrifuged for 10 min at 800×g at 4 °C. The cell pellet was resuspended in 0.9% NaCl solution in order to prepare a 2 % (v/v) cell suspension. One hundred  $\mu$ l of this suspension were plated in each well of a 96-well round bottom plate. The formulated nanosuspension (NF2) solutions of different concentrations (3.90–

500  $\mu$ g/ml) in 0.9% (w/v) in NaCl were added to the plate and incubated for 1 h and 24 h at 37 °C in 5 % CO<sub>2</sub>. The release of haemoglobin, as an index of red blood cell (RBC) lysis (haemolysis), was determined by spectrophotometric analysis of the supernatant at 570 nm. Complete haemolysis (positive control) was achieved by adding 1% (v/v) Triton X-100, while cells in 0.9 % (w/v) NaCl solution served as negative control [33, 34].

#### Statistical analysis

The results were expressed as mean±SD and were analyzed statistically by one-way analysis of variance (ANOVA) using Graph Pad Prism V5.04 software at the level of significance ( $p < 0.05$ ).

## RESULTS AND DISCUSSION

#### Determination of $\lambda$ Max

The analysis of UV spectra of naringenin in, HCl buffer pH 1.2 and Phosphate buffer pH 7.4 shows the same  $\lambda_{max}$  290 nm which similar to the published one as shown in fig. 1. A and 1. B [34].

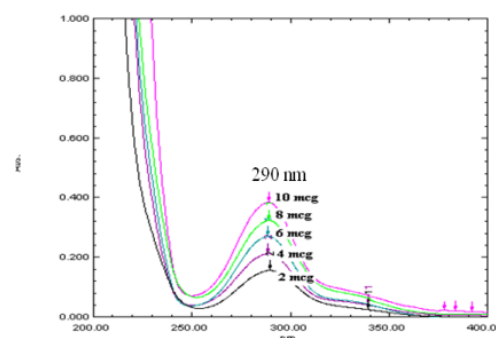


Fig. 1A: UV Spectrum of naringenin in-phosphate buffer pH 7.4

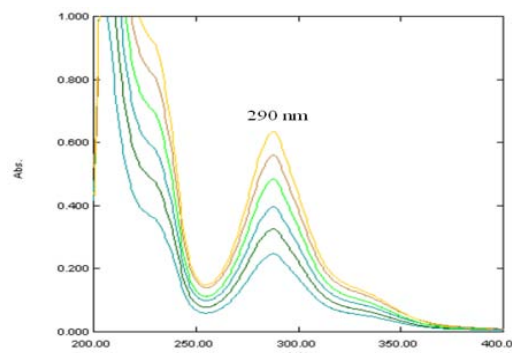


Fig. 1B: UV Spectrum of naringenin in 0.1N HCl pH 1.2

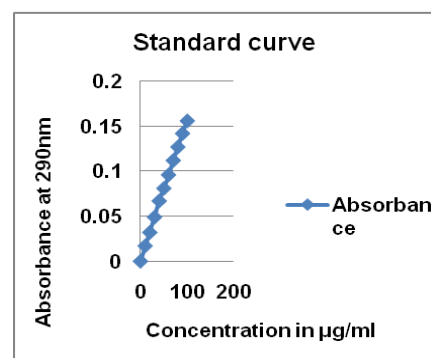
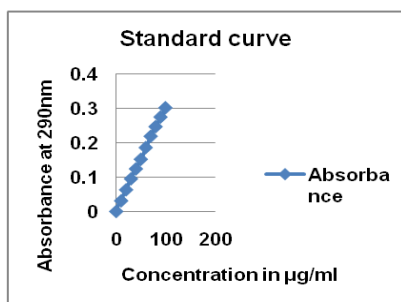


Fig. 2A: Standard curve of naringenin in 0.1N HCl, Regression Coefficient ( $r$ ) = 0.999, Slope ( $b$ ) = 0.00155



**Fig. 2B: Standard curve of naringenin in phosphate buffer, regression coefficient (r) = 0.999, Slope (b) = 0.00303**

### Calibration curves of naringenin

The constructed calibration curves of NAR in HCl buffer pH 1.2 and Phosphate buffer pH 7.4 are shown in fig. 2. A and 2. B. A straight line was obtained by plotting the absorbance versus concentration with a high coefficient of determination. This indicates that the calibration curve obeys Beer's law within the range of concentration used.

### Formulation of nanosuspension

NARNS were prepared by high pressure homogenization using different polymers such as soya lecithin (N1 and N2), Poloxamer 407 (N3 and N4), Poloxamer 188 (N5 and N6), HPMC (N7 and N8) and Tween-80 (N9 and N10) with TPGS respectively. The polymers were selected based on literature review and preformulation studies. The prepared nanosuspension was lyophilized in order to increase the stability [39].

### Particle size analysis and polydispersity index measurement

The effect of particle size and polydispersity index (PDI) was studied using ten different formulations. All the prepared

formulations were in the nano size. The mean particle size (effective diameter) for formulations varied in the narrow range from  $70.89 \pm 0.0$  nm to  $144.5 \pm 0.0$  nm. The particle size and PDI for different formulations are showing in table 2. The choice of suitable stabilizers and its concentration are the most important factors to control the size and stability of our work; Soya lecithin, Polaxamer-407, Polaxamer-188, HPMC, and Tween-80 were used at a different concentration (table 1). The optimum concentration was in the formulation of N1, N2 and N3, which has particle size  $74.37 \pm 0.16$ ,  $80.52 \pm 0.13$  and  $70.89 \pm 0.21$  nm. Also, these formulation shows PDI in the range of  $0.327 \pm 0.05$ ,  $0.284 \pm 0.01$  and  $0.293 \pm 0.09$  and this low value will indicate good stability of the nanosuspension. The results showed that PDI is reduced with the increasing of stabilizer concentration as the PDI of formula N1 which contains 1:0.75:1 of drug: (NAR: Soya lecithin: TPGS) ratio was  $0.327 \pm 0.05$  nm compared with  $0.284 \pm 0.01$  nm for N2 which contains 1:1.5:1 ratio of drug: stabilizer: Co-stabilizer. The reason behind this is that high stabilizer concentration decreases surface tension and stabilizes newly developed surfaces during high-pressure homogenization process and produce nanosuspension of less PDI [35]. Furthermore, low or insufficient concentration of stabilizer will cause instability and recrystallization. TPGS has been shown to improve the bioavailability of many compounds [36]. The combination of TPGS and HPMC in the nanosuspension formulation was shown to inhibit the crystal growth within the system [37]. This could be attributed to the increase in the molar substitution ratio (MSR) of the polymer per drug. The increase of the hydrophilic corona surrounding the polymer to protect the nanosuspension enhances the stability and prevents particles from aggregation. The PDI values were ranged from  $0.284 \pm 0.05$  -  $0.595 \pm 0.16$ , which indicate the acceptable uniformity level for all the prepared formulations [38]. Narrower range of particles sizes will minimize the difference between active agent concentration and the surrounding environment. As a result, the Ostwald ripening phenomenon will be inhibited in nanosuspension during high-pressure homogenization methods [39, 40].

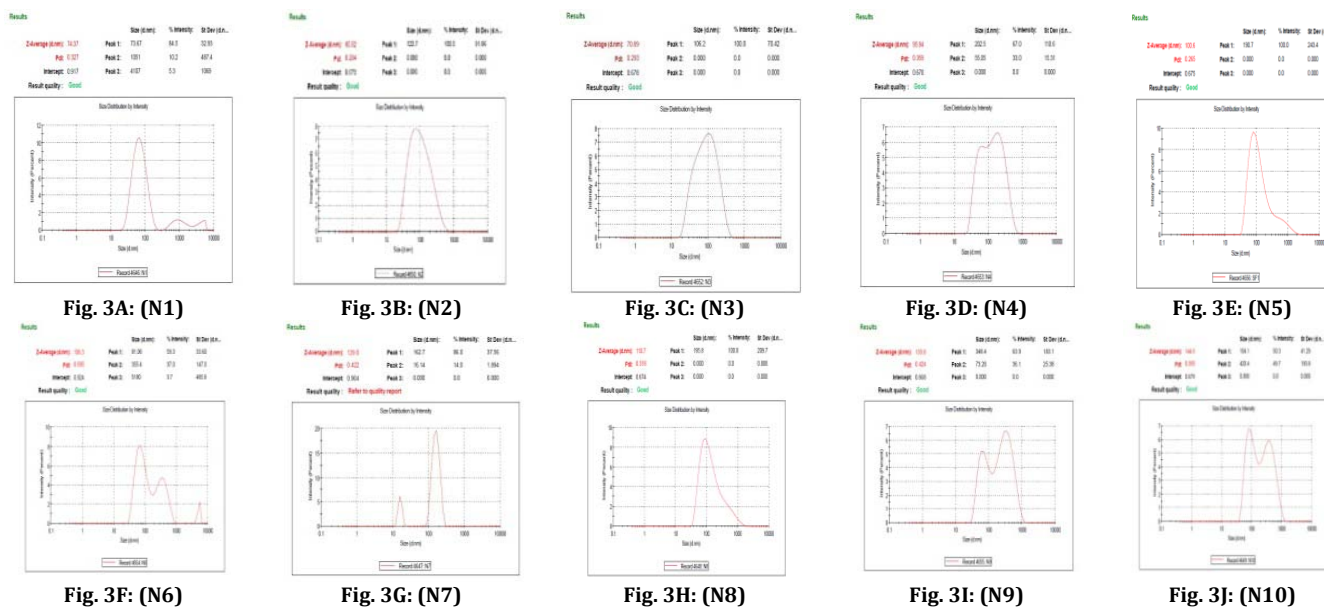


**Fig. 3: Particle size distribution and PDI of nanosuspension formulation**

### Zeta potential

Zeta potential gives certain information on the surface charge properties and furthers the long-term physical stability of the nanosuspension. The zeta potential for the ten formulations of NARNS was shown in fig. 4. The charge was negative due to adsorbed stabilizer and TPGS on the drug particles; so, negative zeta potential is attributed to drug nanosuspension. In general, zeta

potential values of  $\pm 20$  mV are sufficient for the stability of nanosuspension stabilized by the stearic stabilizer. The selected polymers indicating that the prepared formulation would not suffer from instability problems. However, the high zeta potential proposes that the nanosuspension was adequately stabilized. It reflects the electric potential of particles and is influenced by the composition of the particle and the medium in which it is dispersed. The obtained value for selected formulation indicates stable nanosuspension [41].

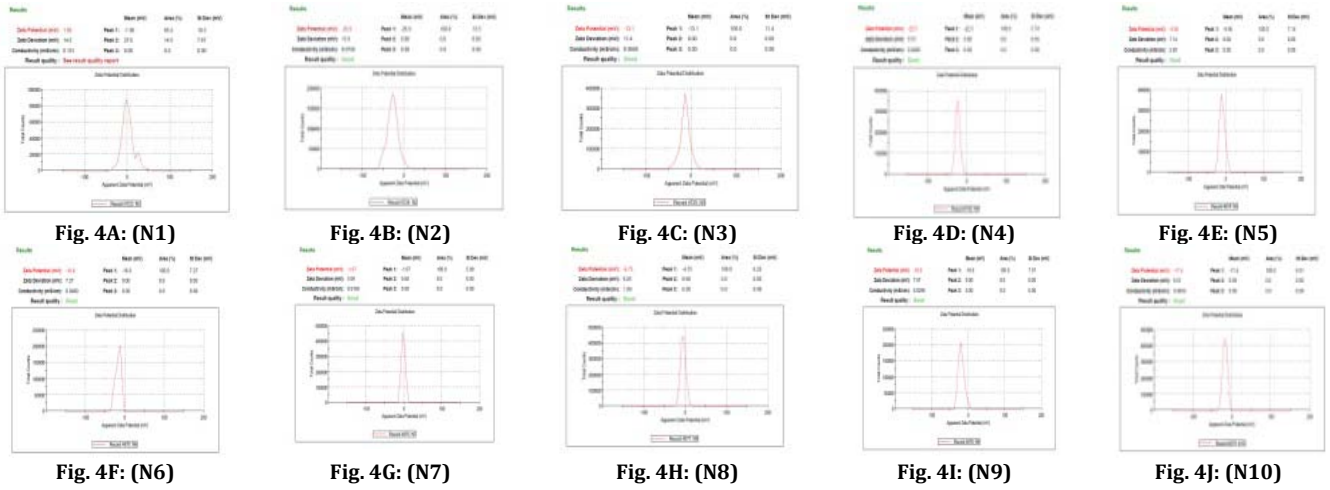


Fig. 4: Zeta potential of NARNS

Table 2: Particle size, polydispersity index, zeta potential, drug content and drug entrapment efficiency of naringenin nanosuspension

S. No.	Formulations	Average particle size (d. nm)	Poly dispersity index (PDI)	Zeta potential (mV)	Drug content	Drug entrapment efficiency (%)
1.	N1	74.37±0.16	0.327±0.05	1.86	95.49±.63	89.0±0.23
2.	N2	80.52±0.13	0.284±0.01	-26.9	98.61±0.32	94.75±0.62
3.	N3	70.89±0.21	0.293±0.09	-13.1	94.73±0.12	88.26±0.86
4.	N4	95.94±0.16	0.359±0.69	-22.5	95.00±0.61	90.12±0.48
5.	N5	100.6±0.28	0.265±0.21	-9.56	91.34±0.56	80.45±0.01
6.	N6	106.3±0.21	0.595±0.16	-16.6	93.48±0.10	84.0±0.48
7.	N7	129.0±0.13	0.422±0.26	-1.67	89.45±0.28	78.56±0.72
8.	N8	110.7±0.64	0.318±0.21	-4.75	90.12±0.92	80.43±0.73
9.	N9	133.8±0.15	0.424±0.16	-18.6	87.34±0.26	73.69±0.73
10.	N10	144.5±0.13	0.393±0.13	-17.4	89.45±0.71	74.37±0.76

Mean of three observation±SD. (n=3)

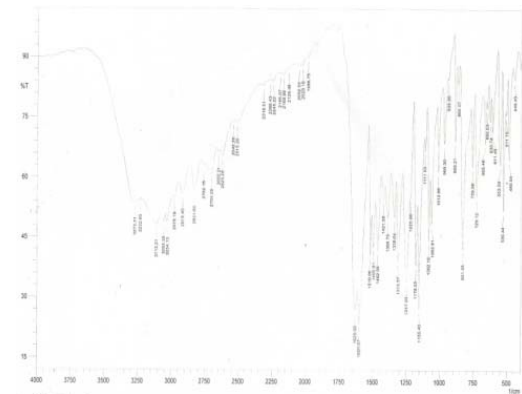


Fig. 5: FTIR spectrum of NAR

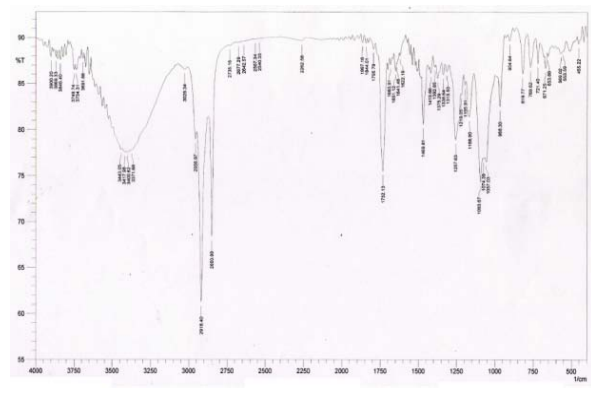


Fig. 6: FTIR spectrum of soya lecithin

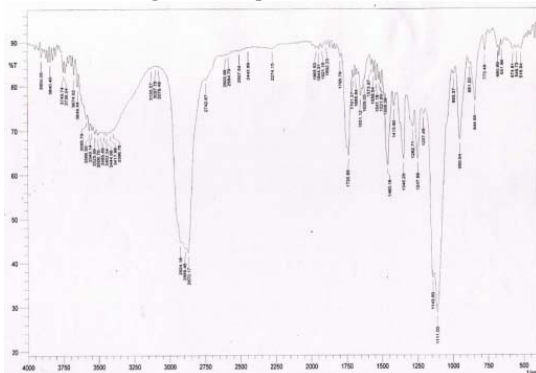


Fig. 7: FTIR spectrum of TPGS

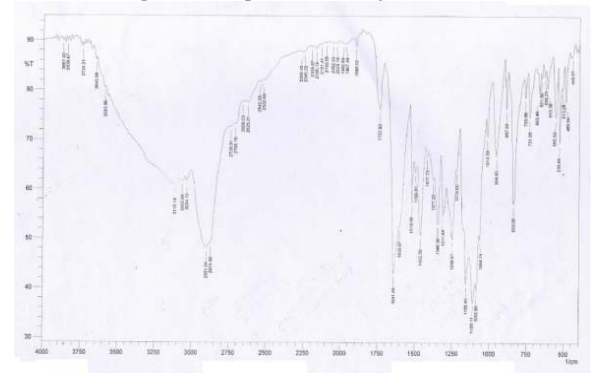


Fig. 8: FTIR spectrum of selected formulation (N2)

### Fourier transforms infrared spectroscopy (FT-IR)

FT-IR spectroscopy is one of the best techniques to evaluate the chemical stability of the encapsulated drug inside the nanosuspension. Fig. 5, 6, 7, 8 shows the FT-IR spectra of free NAR, soya lecithin, TPGS and NARNS. FT-IR spectra confirmed the successful conjugation between NAR and soya lecithin with TPGS at  $\sim 2918.40$  ( $\text{CH}_2$  symmetric stretching) and  $\sim 1707.27$   $\text{cm}^{-1}$  ( $\text{C}=\text{O}$  carbonyl stretching) in NAR-loaded soya lecithin nanosuspension. Free NAR showed the characteristic bands due to the presence of different functional groups. A band appearing at  $\sim 2918.40$   $\text{cm}^{-1}$  is due to  $\text{CH}_2$  asymmetric stretching vibrations while the peak observed at  $\sim 1629.60$   $\text{cm}^{-1}$  is due to  $\text{C}=\text{O}$  stretching respectively. These distinctive bands of free NAR are also present in NARNS, which indicates the chemical stability of NAR in nanosuspensions [42, 43].

### Drug entrapment efficiency

The Percentage drug entrapment efficiency of all the formulations was calculated, and the results were tabulated in table 2. The drug

entrapment efficiency of N2 and N4 was high when compared to other formulations. This may be due to the presence of optimum polymer and TPGS concentrations, comparing the formulations N1, N3, N5, N6, N7, N8, N9, and N10. It is clear that increase in polymer concentration increased the drug entrapment efficiency. Table 2 shows the drug entrapment efficiency of a different formulation of NARNS. The concentration of the stabilizer used is the most effective factor on entrapment efficiency, and this agrees with that obtained by Patil *et al.* who formulate spray dried chitosan nanoparticles containing doxorubicin [44].

### Saturation solubility of freeze-drying nanosuspension

The poor solubility of NAR that determined is in agreement with published researches as shown in table 3, also the results showed that an increase in pH resulted in an increase in the solubility of NAR as showing in the fig. this is because it is an acidic drug ( $\text{pK}_a = 7.91$ ). It was observed that the solubility of prepared NARNS has been increased to  $6.1 \pm 0.2$  folds in pH 1.2 and to  $7.5 \pm 0.4$  folds in pH 7.4 due to the formation of stabilized nanosuspensions and it is shown in fig. 9

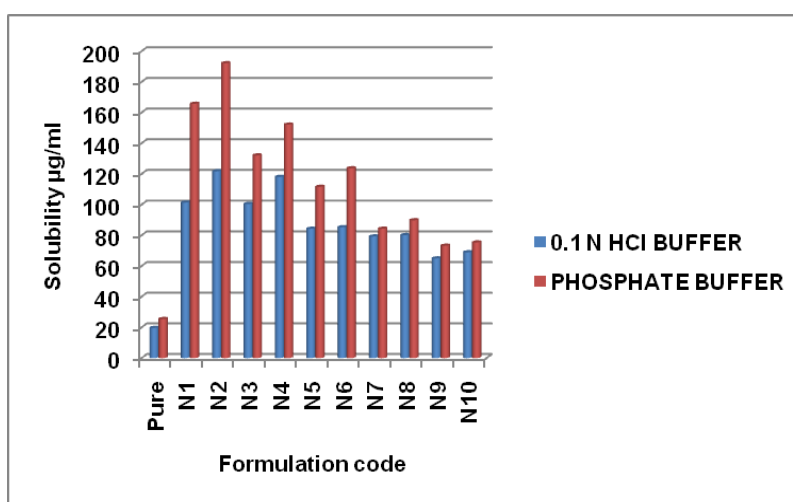


Fig. 9: Saturation solubility studies of NAR and NARNS

### In vitro drug release

*In vitro*, drug release profiles of NAR and NARNS are shown in fig. 10. A and 10. B. The release of NAR and the NARNS of the selected formulation were higher than the release profile of the pure drug in 60 min. The % CDR of the selected formula N2 was more than 90% in twelve h in both

0.1 N HCl and phosphate buffer pH 7.4 media as compared to less than 37.95 % and 24.82 % of NAR in the same media respectively. This will indicate that the dissolution rate of the NARNS is enhanced. Factors that contributing to a fast release was large surface area due to small particle size, high diffusion coefficient (small molecular size), low matrix viscosity and short diffusion distance of the drug [45].

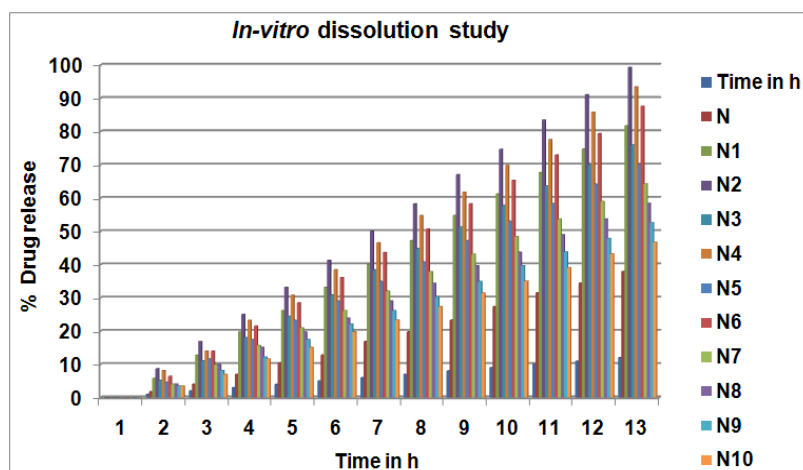


Fig. 10A: Effect of NAR concentration and its NARNS in 0.1N HCl pH 1.2, mean of three observation  $\pm$  SD (n=3)

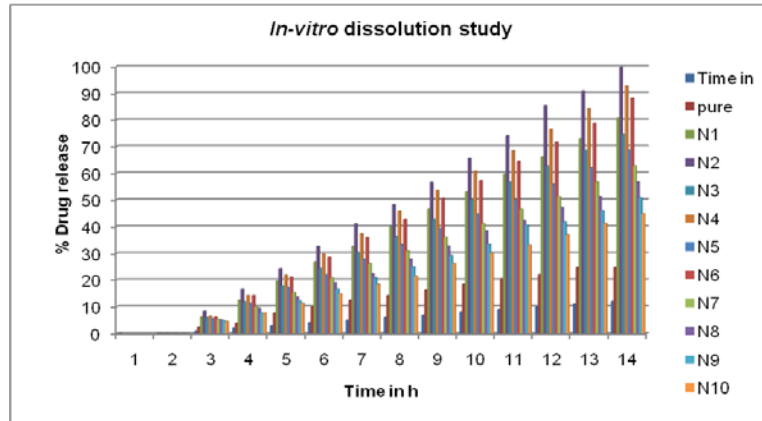


Fig. 10B: Effect of NAR concentration and its NARNS in Phosphate buffer pH 7.4, mean of three observation±SD (n=3)

**In vitro permeability studies**

The *in vitro* permeability study was carried out using Franz Diffusion Cell. After 1 h of diffusion, 97.13 % (N2), of the drug was diffused from the lyophilize nanosuspension, while for NAR, the diffusion was found to be 26.27 % respectively. Thus, the amount of the drug diffused through the nitrocellulose membrane has doubled

when it is given to the form of a nanosuspension. It can be clearly seen that the permeation of the drug from lyophilized NARNS is much faster than the NAR. The enhanced diffusion may be explained in terms of the huge specific surface area of the nanosuspension droplets and improved permeation of the naringenin because of the presence of a surfactant, which reduces the interfacial tension of formulation [46]. The results are shown in fig. 11.

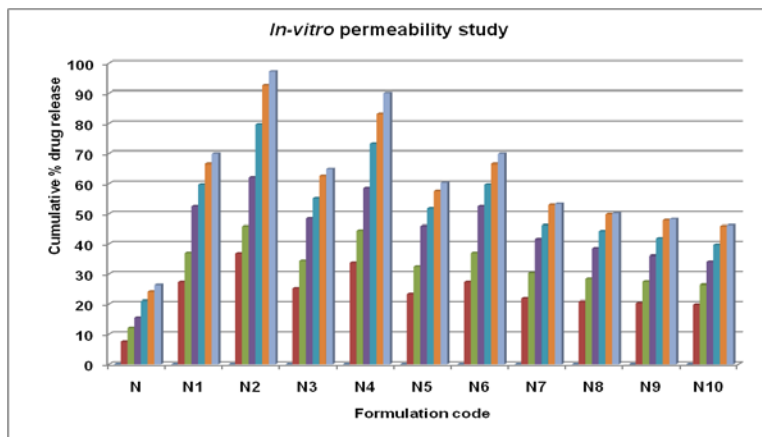


Fig. 11: Comparative permeability studies of NAR and NARNS in phosphate buffer (pH 7.4), mean of three observation±SD. (n=3)

**Scanning electron microscope**

SEM was carried out to study the surface morphology of particles. It was found that NARNS revealed a smooth texture (fig. 12). The SEM picture of NAR particles was found abundantly with larger particle

size when compared to NARNS. Thus, soya lecithin, poloxamer-407, poloxamer 188, HPMC and Tween-80 produced better surface characteristics. The surface structure of nanosuspension in the SEM of N2 appeared good in shape. This micrograph was in agreement with those measured by particle size distribution [47].

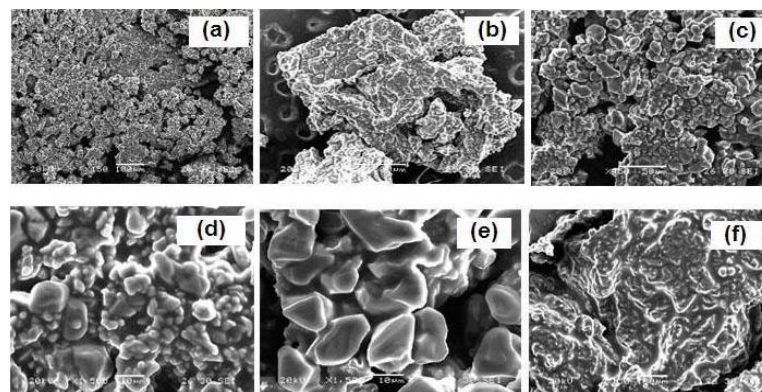


Fig. 12(a): SEM of NAR, 13(b): SEM of Nar-Soya lecithin, 13(c): SEM of Nar-HPMC 13(d): SEM of Nar-poloxamer 188 13(e): SEM of Nar-poloxamer 407 13(f): SEM of Nar-Tween-80

### Powder X-ray diffraction analysis (P-XRD)

A powder X-ray diffraction method is useful tools in identifying the physical nature of the particles. Powder x-ray diffraction patterns of free NAR, polymers and NARNS are present in fig. (13). Free NAR has displayed the characteristic crystalline peaks

of  $2\theta$  of  $10.83^\circ$ ,  $11.49^\circ$ ,  $15.75^\circ$ ,  $17.27^\circ$ ,  $18.07^\circ$ ,  $20.35^\circ$ ,  $23.73^\circ$ ,  $25.37^\circ$ ,  $27.71^\circ$ . However, NARNS has not shown any such crystalline peaks. This absence of detectable crystalline domains of NAR in nanosuspension clearly indicates that NARNS is in amorphous or disordered crystalline phase or in the solid solution state [48].

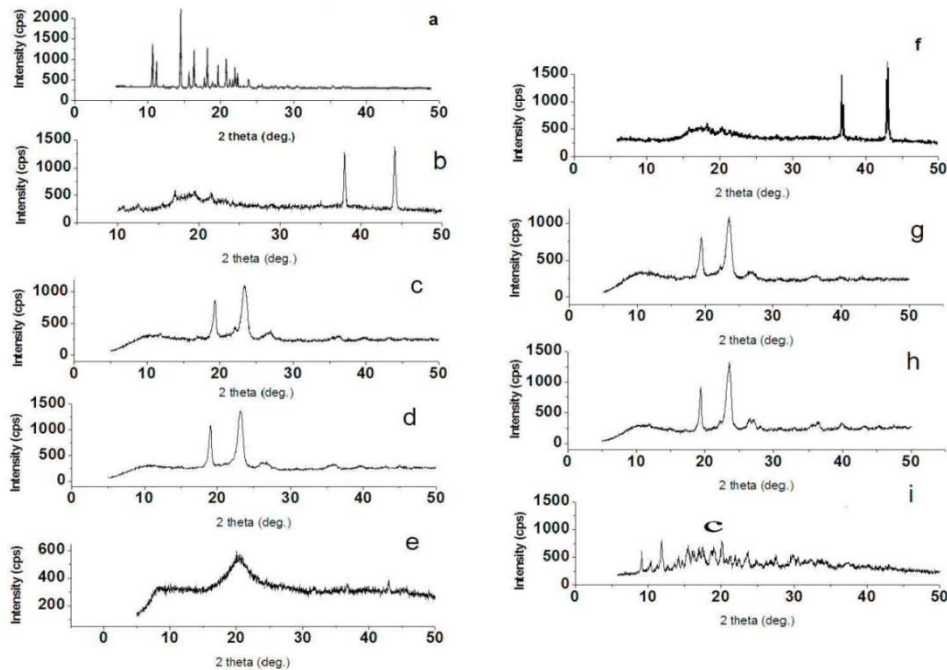


Fig. 13(a): P-XRD of NAR, (b): P-XRD of Soya lecithin, (c): P-XRD of polaxamer-407, (d): P-XRD of Polaxamer-188, (e): P-XRD of HPMC, (f): P-XRD of Nar-Soya lecithin, (g): P-XRD of NAR-Polaxamer-407, (h): P-XRD of NAR-Polaxamer-188, (i): P-XRD of NAR-HPMC

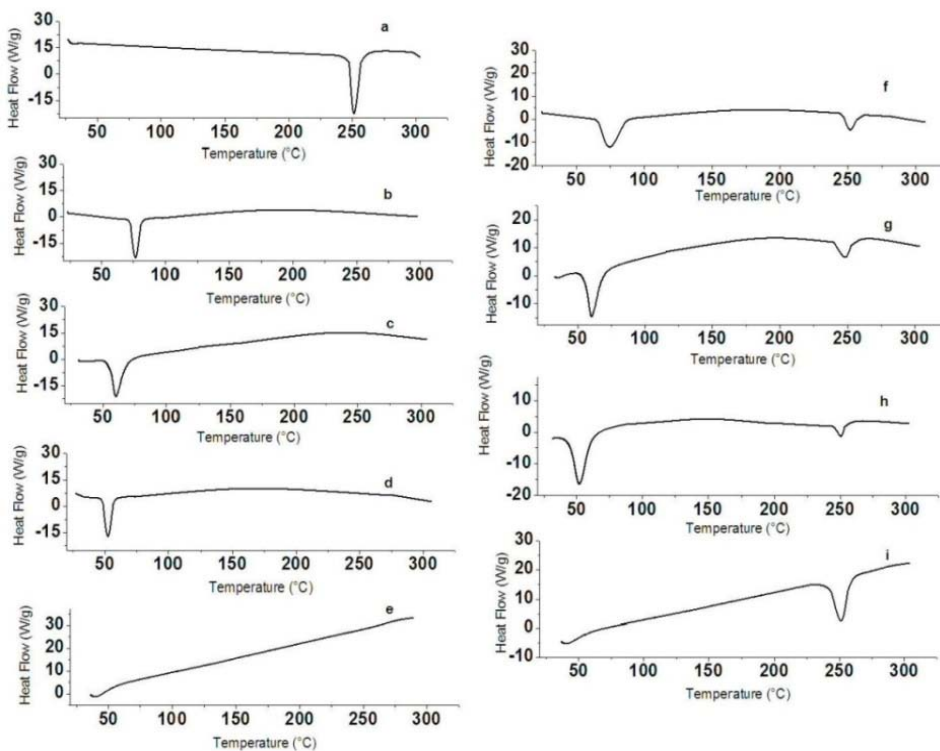


Fig. 14: a: DSC of NAR, (b): DSC of soya lecithin, (c): DSC of polaxamer-407, (d): DSC of polaxamer-188, (e): DSC of HPMC, (f): DSC of Nar-Soya lecithin, (g): DSC of NAR-polaxamer-407, (h): DSC of NAR-polaxamer-188, (i): DSC of NAR-HPMC



### Thermal analysis

DSC was used to elucidate the physical state of the drug within the system. To investigate the molecular state of the drug, DSC study was carried out. The DSC curves of NAR and lyophilized NARNS were recorded. Fig. 14 Shows DSC thermo grams of free NAR, stabilizers and NARNS. Free NAR exhibited a melting endothermic peak around at 250 °C indicating the crystalline nature of the drug. However, NARNS showed broad melting peak indicating the absence of crystalline. Nature of the thermo gram is totally changed, and the sharp peaks are shifted; the peaks of NAR have changed to broad peaks with reduction of the height of each peak. These changes indicate that the dehydration of NAR and change as the particle size

giving a more amorphous type as the product this may help in increasing the dissolution rate of NARNS. Lyophilized NARNS were molecularly dispersed in an amorphous form [49, 50].

### Stability studies

The promising formulation (N2) was subjected to short-term accelerated stability study by storing the formulations at high-density polyethylene bottles and stored at 4±1 °C/Ambient, 25±2 °C/60±5 % RH %, 40±2°C/75±5 % RH for 90 d. After 3 mo, the formulation was again analyzed for drug content. The data for stability studies revealed that there was no considerable difference s in drug content. The Percentage of drug content data is given in table 5.

**Table 5: Stability studies of selected NARNS**

Formulation	Storage temperature condition	Initial drug content (%)	Drug content after 90 d (%)
N2	4 °C	99.52±0.13	99.13±0.41
	Room temperature		99.01±0.91
	40 °C		98.82±0.11

Mean of three observation±SD. (n=3)

### Hemocompatibility assay

Erythrocyte hemolysis test for the formulated drug was conducted. If the hemolysis occurs, the oxyhemoglobin can drain out, and the amount of oxyhemoglobin is linear to the number of blood cells hemolyze. In the study, the rate of erythrocyte hemolysis of distilled water was set as 100% and physiological saline as 0%. The rate of erythrocyte hemolysis of formulated drug (NF2) dramatically

decreased under the current experimental conditions. In general, the hemolysis % was not allowed to be higher than 5% for injection.

The rates of erythrocytes hemolysis for 500–3.90 µg/ml were less of the formulated drug. It demonstrated that the nanosuspension formulation could reduce the damage to erythrocyte membrane effectively, which made this preparation amenable to i. v. injection and circumvented the problem of poor solubility.

**Table 6: Whole blood cell lysis**

S. No.	Concentration (µg/ml)	% hemolysis
1	500	3.4±2.6 *
2	250	2.3±0.7 *
3	125	2.2±0.6 *
4	62.5	1.3±0.9 *
5	31.25	1.1±0.9 *
6	15.62	0.9±1.1 *
7	7.81	0.6±0.9 *
8	3.90	0.4±0.8 *

\*  $p < 0.05$ : % Hemolysis of selected formulation (NF2) using Student's *t*-test. (n=3)

### CONCLUSION

NAR nanosuspension was successfully prepared by high-pressure homogenization technique. This method of manufacturing was found to be simple and has scale-up feasibility. The nanosuspension was converted into dry powder by lyophilization in order to increase its stability. The increase in drug dissolution rate and solubility can be expected to have a significant impact on the oral bioavailability of the drug. The *in vitro* intestinal permeability results showed that the drug diffusion across the intestinal membrane from the NARNS is significantly higher than the NAR suspension. DSC thermogram and P-XRD diffractograms confirmed that the crystalline was converted into amorphous nature after high-pressure homogenization and lyophilization process. Using SEM, it was found that NARNS revealed a smooth texture. The lyophilized NARNS was found to be stable when stored under refrigerated conditions. The hemocompatibility assessment results suggesting the formulated nanosuspension might be a good choice for intravenous administration of poorly soluble NAR. These observations lead us to the conclusion that nanosuspensions seem to be a promising drug delivery system, which can provide an effective and practical solution to the problem of NAR with low aqueous solubility and poor systemic bioavailability. Hence, these results suggest that the NARNS are highly promising cancer drug carrier system with interesting anticancer properties of NAR.

### CONFLICT OF INTERESTS

Declared none

### REFERENCES

- Assi M, Usta J, Mounimne Y, Aboul-Ela M, EL Lakany A. Phytochemical study and the antiproliferative activity of inula vulgaris species grown in lebanon. Int J Pharm Pharm Sci 2017;9:75-83.
- Narain JP, Garg R, Fric A. Non-communicable diseases in the south-east Asia region: burden, strategies and opportunities. Natl Med J India 2011;24:280-7.
- Thun MJ, DeLancey JO, Center MM, Jemal A, Ward EM. The global burden of cancer: priorities for prevention. Carcinogenesis 2010;31:100-10.
- Moorthi C, Manavalan R, Kathiresan K. Nanotherapeutics to overcome conventional cancer chemotherapy limitations. J Pharm Pharm Sci 2011;14:67-77.
- Brewer E, Coleman J, Lowman A. Emerging technologies of polymeric nanoparticles in cancer drug delivery. J Nanomater 2011;1-10. <http://dx.doi.org/10.1155/2011/408675>
- Hollman PCH, Katan MB. Dietary flavonoids: intake, health effects and bioavailability. Food Chem Toxicol 1999;37:937-42.
- Cohen J, Kristal A, Stanford J. Fruit and vegetable intakes and prostate cancer risk. J Natl Cancer Inst 2000;92:61-8.
- Birt DF, Hendrich S, Wang W. Dietary agents in cancer prevention: flavonoids and isoflavonoids. Pharmacol Ther 2001;90:157-77.
- Kris-Etherton PM, Hecker KD, Bonanome A, Coval SM, Binkoski AE, Hilpert KF, Griel AE, et al. Bioactive compounds in foods: their role in the prevention of cardiovascular disease and cancer. Am J Med 2001;113:71-88.

10. Verhoeven ME, Bovy A, Collins G, Muir S, Robinson S, Colliver S, *et al.* Increasing antioxidant levels in tomatoes through modification of the flavonoids biosynthetic pathway. *J Exp Bot* 2002;53:2099–106.
11. Bugianesi R, Salucci M, Leonardi C, Ferracane R, Catasta G, Azzini E, *et al.* Effect of domestic cooking on human bioavailability of naringenin, chlorogenic acid, lycopene and beta-carotene in cherry tomatoes. *Eur J Nutr* 2004;43:360-6.
12. Kawaii S, Tomono Y, Katase E, Ogawa K, Yano M. Quantitation of flavonoids constituents in citrus fruits. *J Agric Food Chem* 1999;47:3565–71.
13. Frydoonfar HR, McGrath DR, Spiegelman AD. The variable effect on proliferation of a colon cancer cell line by citrus fruit flavonoid naringenin. *Colorectal Disease* 2002;5:149–52.
14. Virgili F, Acconcia F, Ambra R, Rinna A, Totta P, Marino M. Nutritional flavonoids modulate estrogen receptor a signaling. *IUBMB Life* 2004;56:145–51.
15. Monica Kristiani, Sismindari, Ronny Martien, Hilda Ismail, Agustinus Yuswanto. Cytotoxic activity of acidic ribosome inactivating proteins mirabilis Jalapa L. (Rip Mj-C) nanoparticle formulated with low-chain chitosan and low-methylated pectin. *Int J Pharm Pharm Sci* 2017;9:69-74.
16. Mustafa R, Abdulbaqi. Evaluation the effect of nanotechnology on pharmaceutical and biological properties of metronidazole. *Int J Pharm Pharm Sci* 2017;9:139-45.
17. Kunal S, Ravindra B. UV spectrophotometric method for the estimation of azilsartan medoxomil in bulk and pharmaceutical formulations. *World J Pharm Res* 2015;4:1667-72.
18. Gandhi S, Mittal P, Pahade A, Rege S. Development and validation of stability indicating HPTLC method for estimation of azilsartan medoxomil. *Pharm Sci Monitor* 2015;6:224-32.
19. Lina Winarti, Lusia Oktora Ruma Kumala Sari, Agung Endro Nugroho. Naringenin-loaded chitosan nanoparticles formulation and its *in vitro* evaluation against t47d breast cancer cell line. *Indonesia J Pharm* 2015;26:145-57.
20. Sun M, Gao Y, Pei Y, Guo C, Li H. Development of nanosuspension formulation for oral delivery of quercetin. *J Biomed Nanotechnol* 2010;6:325-32.
21. Kidambi S, Yarmush RS, Novik E, Chao P, Yarmush ML, *et al.* Oxygen-mediated enhancement of primary hepatocyte metabolism, functional polarization, gene expression, and drug clearance. *Proc Natl Acad Sci USA* 2009;106:15714–9.
22. Huong DT, Takahashi Y, Ide T. Activity and mRNA levels of enzymes involved in hepatic fatty acid oxidation in mice fed citrus flavonoids. *Nutrition* 2006;22:546–52.
23. Rajalakshmi R, Venkataramudu T, Kumar R, Divya K, Kiranmayi M. Design and characterization of valsartan nanosuspension. *Int J Pharmacother* 2012;2:70-81.
24. Kroyer G. The antioxidant activity of citrus fruit peels. *Z. Ernahrungswiss* 1986;25:63–9.
25. Prakash S, Vidyadhara S, Sasidhar RLC, Abhijit D, Akhilesh D. Development and characterization of Ritonavir nanosuspension for oral use. *Pharm Lett* 2013;5:48-55.
26. Sahu BP, Das MK. Nanosuspension for enhancement of oral bioavailability of felodipine. *Appl Nanosci* 2013;4:1-9.
27. Kanaze FI, Bounartzi MI, Georgarakis M, Niopas I. Pharmacokinetics of the citrus flavanone aglycones hesperetin and naringenin after single oral administration in human subjects. *Eur J Clin Nutr* 2007;61:472-7.
28. Kunal S, Ravindra B. UV spectrophotometric method for the estimation of azilsartan medoxomil in bulk and pharmaceutical formulations. *World J Pharm Res* 2015;4:1667-72.
29. Yuancai D, Wai KN, Jun H, Shoucang S, Reginald BHT. A continuous and highly effective static mixing process for antisolvent precipitation of nanoparticles of poorly water-soluble drugs. *Int J Pharm* 2010;386:256–61.
30. Dubhi M, Ghodasara U, Mori D, Patel K, Manek R, Sheth NR. Formulation, optimization and characterization of candesartan cilexetil nanosuspension for *in vitro* dissolution enhancement. *Afr J Pharm Pharmacol* 2015;9:102-13.
31. Ige PP, Baria RK, Gattani SG. Fabrication of fenofibrate nanocrystals by probe sonication method for enhancement of dissolution rate and oral bioavailability. *Colloids Surf B* 2013;108:366–73.
32. Natarajan Jawahar, Subramanya Nainar Meyyanathan, Venkatachalam Senthil, Kuppusamy Gowthamarajan, Kannan Elango. Studies on physicochemical and pharmacokinetic properties of olanzapine through nanosuspension. *J Pharm Sci Res* 2013;5:196–202.
33. Mahendra Nakarani, Priyal Patel, Jayvadan Patel, Pankaj Patel, Rayasa S, R Murthy, *et al.* Cyclosporine a-nanosuspension: formulation, characterization and *in vivo* comparison with a marketed formulation. *Sci Pharm* 2010;78:345-61.
34. Liqin Zhang, Li Song, Peipei Zhang, Tingting Liu, Li Zhou, Guangde Yang, *et al.* Solubilities of naringin and naringenin in different solvents and dissociation constants of naringenin. *J Chem Eng Data* 2015;60:932–40.
35. McClements D. Crystals and crystallization in oil-in-water emulsions: implications for emulsion-based delivery systems. *Adv Colloid Interface Sci* 2012;174:1-30.
36. Ghosh I, Snyder J, Vippagunta R, Alvine M, Vakli R, Tong W. Comparison of HPMC based polymers performance as carriers for the manufacture of solid dispersions using the melt extruder. *Int J Pharm* 2011;419:12–9.
37. Rajebahadur M, Zia H, Nues A, Lee C. Mechanistic study of solubility enhancement of nifedipine using vitamin E TPGS or solutol HS-15. *Drug Delivery* 2006;13:201–6.
38. Helgason T, Awad TS, Kristbergsson K, McClements DJ, Weiss J. Effect of surfactant surface coverage on formation of solid lipid nanoparticles (SLN). *J Colloid Interface Sci* 2009;334:75-81.
39. Van Eerdenbrugh B, Vermant J, Martens JA, Froyen L, Van Humbeeck J, Augustijns P. A screening study of surface stabilization during the production of drug nanocrystals. *J Pharm Sci* 2009;98:2091-103.
40. Merisko-Liversidge E, Sarpotdar P, Bruno J, Hajj S, Wei L, Peltier N. Formulation and antitumor activity evaluation of nanocrystalline suspensions of poorly soluble anticancer drugs. *Pharm Res* 1996;13:272-8.
41. Müller RH, Jacobs C, Kayser O. Nanosuspension as particulate drug formulations in therapy rationale for development and what we can expect for the future. *Adv Drug Delivery Rev* 2001;47:3–19.
42. Sahu SK, Mallick SK, Santra S, Maiti TK, Ghosh SK, Pramanik P. *In vitro* evaluation of folic acid modified carboxymethyl chitosan nanoparticles loaded with doxorubicin for targeted delivery. *J Mater Sci Mat Med* 2010;21:1587-97.
43. Misra R, Sahoo SK. Intracellular trafficking of nuclear localization signal conjugated nanoparticles for cancer therapy. *Eur J Pharm Sci* 2010;39:152-63.
44. Patil P, Bhoskar M. Optimization and evaluation of spray dried chitosan nanoparticles containing doxorubicin. *Int J Curr Pharm Res* 2014;6:7-15.
45. Jose Raul Medina, Mariel Cortes, Erik Romo. Comparison of the USP apparatus 2 and 4 for testing the *in vitro* release performance of ibuprofen generic suspensions. *Int J Appl Pharm* 2017;9:90-5.
46. Dixit P, Jain DK, Dumbwani J. Standardization of an *ex vivo* method for determination of intestinal permeability of drugs using everted rat intestine apparatus. *J Pharmacol Toxicol Methods* 2012;65:13-7.
47. Mou D, Chen H, Wan J, Xu H, Yang X. Potent dried drug nanosuspensions for oral bioavailability enhancement of poorly soluble drugs with pH-dependent solubility. *Int J Pharm* 2011;413:237-44.
48. Mahapatra A, Murthy P. Solubility and dissolution rate enhancement of efavirenz by inclusion complexation and liquid anti-solvent precipitation technique. *J Chem Pharm Res* 2014;6:1099-106.
49. Naguib YW, Rodriguez BL, Li X, Hursting SD, Williams RO, Cui Z. Solid lipid nanoparticle formulations of docetaxel prepared with high melting point triglycerides: *in vitro* and *in vivo* evaluation. *Mol Pharm* 2014;11:1239–49.
50. Li J, Guo X, Liu Z. Preparation and evaluation of charged solid lipid nanoparticles of tetrandrine for ocular drug delivery system: pharmacokinetics, cytotoxicity and cellular uptake studies. *Drug Dev Ind Pharm* 2014;40:980–7.

51. Kim CK, Kim JH, Park KM, Oh KH, Oh U, Hwang SJ. Preparation and evaluation of a titrated extract of centella asiatica injection in the form of an extemporaneous micellar solution. *Int J Pharm* 1997;146:63-70.
52. Xiong R, Lu W, Li J, Wang P, Xu R, Chen T. Preparation and characterization of intravenously injectable nimodipine nanosuspension. *Int J Pharm* 2008;350:338-43.